Dominant energetics in multi-component bio-molecular condensates

Daoyuan Qian,[1] Hannes Ausserwoger,[1] Tomas Sneideris,[1] Mina Farag,[2] Rohit V. Pappu,[2] and Tuomas P. J. Knowles[1,3,†]

[1] *Centre for Misfolding Diseases, Yusuf Hamied Department of Chemistry, University of Cambridge, Lensfield Road, Cambridge, CB2 1EW, UK*

[2] *Department of Biomedical Engineering and Center for Biomolecular Condensates, Washington University in St. Louis, St. Louis, MO 63130, USA*

[3] *Cavendish Laboratory, Department of Physics, University of Cambridge, J J Thomson Ave, Cambridge, CB3 0HE, UK*

The condensation of bio-molecules into membrane-less organelles has been shown to be integral to biological function and malfunction in living cells. These condensed phases typically contain many different molecular components which can all interact with each other. A fundamental challenge with such systems, therefore, is to identify and estimate out of all possible intermolecular interactions the ones which drive the process. Here we address this challenge by developing and determining from experimental data a dominance parameter D^α for each solute α in a multi-component system. This parameter elucidates what fraction of the total free energy change upon phase separation is associated with interactions with each solute, and can be estimated using simple experimental methods. In addition, under the assumption that all solutes contribute energetically favourably to the phase separation process, the theory predicts that modulators that drive phase separation preferentially partition inside condensates, and vice versa. Our formulation does not assume a specific form of the free energy or the number of solute components, allowing the framework to be applied to study energetics in a wide range of phase separation systems.

The general principle of liquid-liquid binary phase separation is simple: starting from a single mixed solution state, the solutes de-mix to form two compartments with distinct compositions to lower the system's total free energy. The two compartments formed have equal chemical potentials and osmotic pressure, as required by phase equilibria [1]. This process is the theoretical underpinning of bio-molecular condensate formation [2–4], which has been shown to play important roles in cellular physiology [5–9] and also diseases [10, 11]. In order to understand and eventually utilise this condensation process it is imperative to identify and estimate key intermolecular interactions in each system. A central approach is to solve for the phase boundary and compare that with experimental results, using techniques such as Field-Theoretic Simulation [12], numerical computation with a model free energy density [13, 14], and coarse-grained simulation that allow residue-level interaction energies to be fitted with Bayesian optimisation [15, 16]. These attempts have led to promising results, but a major hurdle now lies in generalising a single method to all phase separation systems. Presently, each method has their own assumptions regarding conditions that are difficult to model explicitly such as pH and salt, while in reality these ignored solute dimensions can have major impacts on the phase separation process [17–20] so mechanistic information can be lost due to this oversight. Notably, the macromolecule polyethylene glycol (PEG) has traditionally been used by the bio-molecular condensate field as an inert crowder [11, 21] but it is increasingly clear that PEG is acting as an associative linker that partitions inside condensates [22–24], instead of staying in the dilute phase to exert an osmotic pressure. It is thus important to decipher which solutes are 'dominant' before any modelling attempt is made, while how to do so has remained a mystery so far. The challenge is then to develop a flexible analysis framework with as few assumptions as possible, such that a wide range of systems can be studied in a consistent manner.

Here we address this challenge by considering a phase separation system of an arbitrary number N of solute components forming two distinct phases, and investigating the relationship between accessible experimental observables and the underlying thermodynamics. We do not assume any specific form of the free energy density, and instead ask what information we can gain from simply analysing experimental data. We found that near the dilute phase boundary, the free energy change associated with one solute relative to the whole system is closely linked to the phase boundary shape, tie lines, and dilute phase solute concentrations, so we define the dominance of a solute as this free energy fraction. We first demonstrate the flexibility and utility of the dominance parameter by analysing data from already published 2-component simulations, and by comparing the dominance trend with those generated from simplistic Flory-Huggins models we further deduce the relative interaction strengths that are consistent with the data. In the second half of the paper we show that a simple dominance measurement approach exists for multi-component cases that can be adapted to any system of interest. In addition, we outline practical interpretations of dominance values in the context of modulations of interactions driving phase separation. The dominance framework is a new path towards quantitative investigations of phase separation systems and

† tpjk2@cam.ac.uk

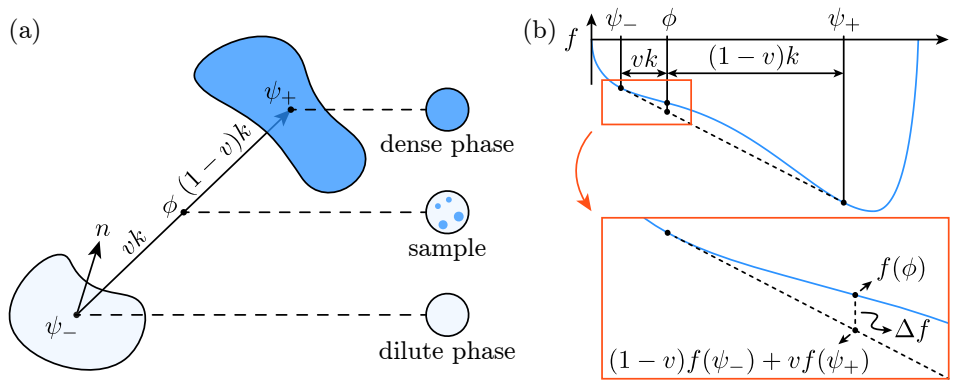

FIG. 1. (a) The full N-D phase space consists of dilute (light blue) and dense (dark blue) phase binodal boundaries, tie lines k^α connecting them, and dilute boundary surface normals n_α. (b) The free energy before and after phase separation is $f(\phi)$ and $(1-v)f(\psi_-)+vf(\psi_+)$ respectively, and a 1-D representation is used here but this is generalisable to any number of dimensions.

the simple experimental approach makes it accessible to most laboratories.

Defining dominance as an energetic measure

We denote the total concentrations of solutes in a sample as ϕ^α where $\alpha = 1, 2, \ldots, N$. The dilute and dense phase boundaries can be represented by two $(N-1)$-D surfaces in the N-D concentration space, and we use ψ_-^α and ψ_+^α to denote solute concentrations on the dilute and dense surfaces respectively. Mass balance requires that for each sample ϕ^α, the line connecting ψ_-^α and ψ_+^α at equilibrium passes through ϕ^α. We define the tie line vector $k^\alpha \equiv \psi_+^\alpha - \psi_-^\alpha$ and use v to denote the volume of the dense phase relative to the whole system. The mass balance equation can then be written as $\phi^\alpha = \psi_-^\alpha + vk^\alpha$. Furthermore, we use n_α to denote the vector normal to the dilute phase boundary, defined by $\sum_{\alpha=1}^N n_\alpha \delta\psi_-^\alpha = 0$ with $\delta\psi_-^\alpha$ a vector lying on the dilute phase boundary. This construction of the phase space is entirely geometrical and the only assumption is that two phases co-exist at equilibrium (Figure 1a). To fully define the space we in principle need to assign a metric $g^{\alpha\beta}$ that connects the units of different solute concentrations, and a natural choice is to use the volume fraction of solutes as a fundamental unit of measure. This in turn allows a 'distance' to be defined this space but we observe below that neither the metric nor the distance is relevant in connecting the thermodynamics to experimental observables, so we omit discussions of these subtleties from the present work. Summation of indices are also explicitly written out in the main text.

Phase separation occurs because the total free energy density of the system decreases upon de-mixing, and we denote this free energy density difference by $\Delta f < 0$ (Figure 1b). We write the energy density $f(\phi)$ of a system as a function of volume fractions of solutes ϕ^α, and since the volume is constrained in defining ϕ^α, $f(\phi)$ corresponds to the Helmholtz free energy. Under the assumption that the volume occupied by a molecule is a constant in the phase separation process, it can be shown that $f(\phi)$ also plays the role of the Gibbs free energy per molecule, so the theoretical results here can be applied to practical systems where the pressure, instead of volume, is held constant (SI section I). We compute Δf and by limiting the dense phase volume relative to the whole system v to be small, equivalent to probing regions close to the dilute phase boundary, Δf is given by (SI section II)

$$\Delta f = -\frac{1}{2}\sum_{\alpha=1}^{N}\sum_{\beta=1}^{N} vk^\alpha vk^\beta \partial_\beta \mu_\alpha(\psi_-) + \mathcal{O}(v^3) \quad (1)$$

where the chemical potential is $\mu_\alpha(\phi) \equiv (\partial_\alpha f)|_\phi$. Since $vk^\alpha = \phi^\alpha - \psi_-^\alpha$ represents the phase space displacement of the total composition from the dilute composition, the sum over β can be viewed as computing the change in chemical potential of solute α under phase separation. As such we define the individual term

$$\Delta f^\alpha \equiv -\frac{1}{2} vk^\alpha \sum_{\beta=1}^{N} vk^\beta \partial_\beta \mu_\alpha(\psi_-) \quad (2)$$

and it quantifies the free energy change associated with the partitioning of solute α. We are interested in the ratio $\lim_{v\to 0}\frac{\Delta f^\alpha}{\Delta f}$, corresponding to the relative energetic contribution of solute α at the onset of phase separation, and define the dominance of α to be

$$D^\alpha \equiv \lim_{v\to 0}\frac{\Delta f^\alpha}{\Delta f} = \frac{\sum_{\beta=1} k^\alpha k^\beta (\partial_\alpha \partial_\beta f)|_{\psi_-}}{\sum_{\gamma=1}^N \sum_{\sigma=1}^N k^\gamma k^\sigma (\partial_\gamma \partial_\sigma f)|_{\psi_-}} \quad (3)$$

so that for each point ψ_-^α on the dilute phase boundary a D^α can be calculated. Notice that D^α is dimensionless and the sum over all solutes is $\sum_\alpha^N D^\alpha = 1$, and it is possible to deduce the relative 'importance' of a solute compared to others, thus the name 'dominance'. Intuitively, if D^α for a solute α is found to be close to 1 in a system, this implies $D^{\alpha'} \approx 0$ for $\alpha' \neq \alpha$ and the system is effectively single-component. On the other

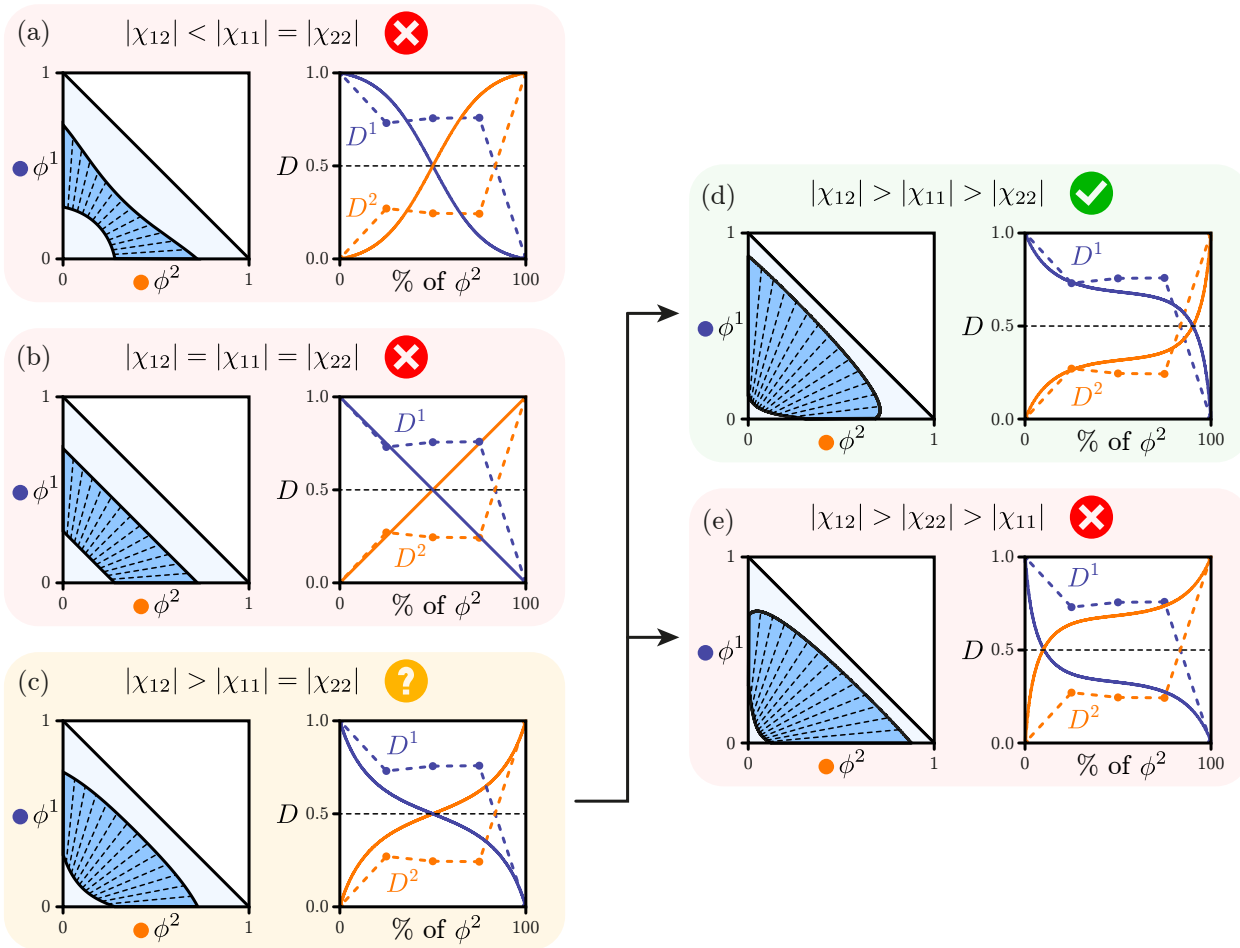

FIG. 2. Computationally generated 2-D phase diagrams from the Flory-Huggins model (left panels) and dominance values of the two solutes (right panels). Dominance values calculated from simulations in [16] are scatter points connected by dashed lines. In (a), (b) and (c) the homotypic interactions are the same, and the heterotypic interaction is weaker than, the same as, or stronger than the homotypic interactions respectively. Comparing the dominance trend to the A1/FUS system suggests the heterotypic interaction is likely stronger than homotypic attractions, and by further varying one of the homotypic interactions in (d) and (e) we deduce the homotypic interaction among ϕ^1 is stronger than that among ϕ^2.

hand, for a multi-component system, we expect D^α to be in the range of (0,1) for two or more solutes. D^α can thus serve as a way to quantify the multi-component character of solutes in a system.

Dominance computation from phase diagrams

Having formulated the dominance D^α we next explore how it can be computed from experimental observables. We motivate the derivation by taking simulation data from [16], where a phase separation system consisting of Low-Complexity Domains of protein Fused in Sarcoma (FUS-LCD) and protein hnRNPA1 (A1-LCD) was studied. Both FUS-LCD and A1-LCD phase separate on their own, and by mixing them at different ratios while keeping their total concentration the same, a 2-D phase diagram with tie lines can be produced. Ratios between n_α's and k^α's can thus be computed using the gradient of the phase boundary and tie lines. The simulation results are reproduced in *in vitro* experiments, revealing strong heterotypic attraction between these proteins [16]. The simulation represents an exact 2-D system, and to obtain estimates for the dominance values for the polymers we note that the tie line vector k^α already appears in Eq. (1), so we focus on the phase boundary normal n_α. By perturbing the equilibrium compositions we arrive at $n_\alpha \propto \sum_{\beta=1}^{N} k^\beta (\partial_\alpha \partial_\beta f)|_{\psi_-}$ (SI section III) and direct substitution and comparison with Eq. (3) establishes the relationship between D^α and the geometrical quantities

$$D^\alpha = \frac{n_\alpha k^\alpha}{\sum_{\gamma=1}^{N} n_\gamma k^\gamma}. \tag{4}$$

In the case of a 2-D system as in [16] we simply have $\alpha = 1, 2$, and we use index 1 to denote A1-LCD

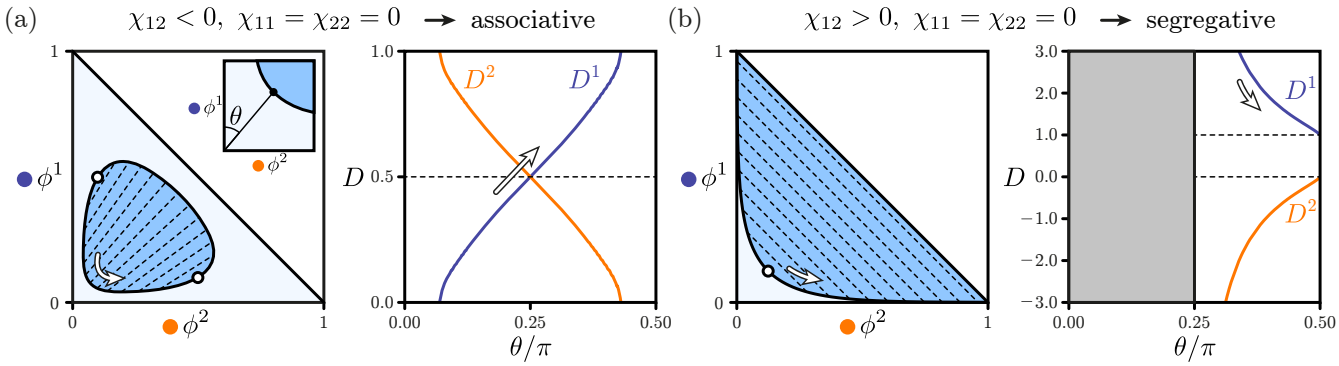

FIG. 3. When phase-separation is driven purely by heterotypic interactions, both attraction (e) and repulsion (b) can lead to de-mixing. Left panels show the 2-D phase diagrams with white points as critical points, and computed D^α values are plotted in the right panels. Inset: θ is defined as the angle formed between the dilute phase point where the dominance is evaluated, and the ϕ^1 axis. As the point of evaluation approaches the critical points (black arrows) the D^α values encounter a singularity as Δf goes to 0. An interesting observation in (b) is that here, D^1 takes on values not in the range of $(0, 1)$, reflecting the abnormal behaviour of a repulsion-driven phase-separating system.

and 2 for FUS-LCD. The tie line gradient k^1/k^2 and the gradient of the phase boundary $-n_2/n_1$ can be combined to give the ratio $D^1/D^2 = (n_1/n_2)(k^1/k^2)$, and using $D^1 + D^2 = 1$ we obtain individual estimates of D^1 and $D^2 = 1 - D^1$. The simulation in [16] was performed with a constant total concentration of A1-LCD and FUS-LCD, and 5 samples were simulated with varying percentages of each protein. Plotting the dominance of A1-LCD as a function of % of FUS-LCD shows that when both proteins are present in the system, the dominance of A1-LCD is consistently larger than that of FUS-LCD (Figure 2, scatter points and dashed lines), and the dominance values are trivially 0 or 1 when either protein is absent from the system.

To elucidate the relative interaction strengths in the simulation system we use a 2-component Flory-Huggins model [25, 26] to generate the full phase diagram of a simplified system through the convex hull algorithm [13, 27, 28] (Appendix IV). In our computation we assume the two solutes are of unit length, fix the total $\phi^1 + \phi^2$ concentration to be 0.5, and compute their dominance parameters as a function of % of ϕ^2 just like in [16]. All interaction parameters are negative, so both solutes attract each other. We first fix the homotypic interactions χ_{11} and χ_{22} to be the same and vary the heterotypic interaction χ_{12} to be weaker than (Figure 2a), the same as (Figure 2b), or stronger than (Figure 2c) the homotypic interaction. The dominance values for the former two cases vary rapidly as % of ϕ^2 increases, qualitatively different from the data trend, so we deduce the heterotypic interaction is stronger than the homotypic interactions, as also suggested in the original paper [16]. To further estimate the relative strengths of the two homotypic interactions, we make χ_{11} to be stronger (Figure 2d) or weaker (Figure 2e) than χ_{22}. The dominance trend produced in the former case is qualitatively very similar as that observed in the simulation data, and we conclude that not only is the heterotypic attraction the strongest, the homotypic attraction among A1-LCD is stronger than that among FUS-LCD. It is worth noting that the dilute phase boundary from simulations is orders of magnitude smaller than in the Flory-Huggins computation, while the dimensionless nature of D^α means this difference can be ignored and only important features of the phase space, including the phase boundary gradient and the tie lines, are relevant.

Having examined the case where homotypic interactions can drive phase separation, we next study a very different scenario where the phase-separation is driven purely by the heterotypic interaction. We set $\chi_{11} = \chi_{22} = 0$ and as established before [22], phase-separation can happen with either strong heterotypic attraction (Figure 3a) or heterotypic repulsion (Figure 3b) in the absence of any homotypic interaction. In presenting dominance values we also use a different parameterisation: for each point on the dilute phase boundary we compute the angle θ made between the vector connecting the origin to that point and the ϕ^1 axis, and plot D^α as a function of θ. This is qualitatively the same as plotting D^α as a function of % of ϕ^2 except in the segregative case, where the negative tie line gradient means D^α stay constant if the total solute concentration is fixed. Repeating the D^α calculation now gives drastically different results. With strong heterotypic attraction (Figure 3a), the computed D^1 starts off at a small value and increases as more ϕ^2 is added. This effect is of entropic origin: at low ϕ^2, the translational entropy of ϕ^2 acts as the main free energy barrier against phase-separation, and as ϕ^2 increases this barrier rapidly diminishes in size due to the logarithmic scaling of the entropic free energy. The interaction free energy is however only changing slowly, so the interaction free energy previously counterbalanced by

the entropic free energy is suddenly released. Consequently, the free energy release by ϕ^2 is more significant compared to that by ϕ^1 and thus D^2 attains a much larger value than D^1. Conceptually, the dominance then also reflects which solute is 'limiting' in the phase separation process. With heterotypic repulsion (Figure 3b), defining dense and dilute phases is non-trivial because the solutes partition into separate phases. Here we focus on the region of phase space where $\theta > \pi/4$ so that the dense phase is higher in ϕ^1. In this region, $D^1 > 1$ throughout and this implies $D^2 = 1 - D^1 < 0$. This can appear counter-intuitive, as it appears that ϕ^2 is in an energetically less favourable state after phase-separation. This is explained by the fact that by phase-separating, the change in chemical potential of ϕ^1 due to partitioning of ϕ^2 releases much more free energy to balance out the unfavourable contribution from ϕ^2 itself, and thus ϕ^2 is acting as a 'sacrificial' component. This behaviour is expected of real crowders [19, 29] but has so far not been observed in bio-molecular condensate systems. It is also worth noting that in both cases, as the system moves towards a critical point, D^1 appears to approach a singularity and this arises because at the critical point, $\Delta f = 0$ and the dominance becomes ill-defined.

Motivated by the computational models, we outline experimental insights that can be gained if multiple solutes can be measured post phase separation. If D^α and ratios of n_α and k^α can be measured at each experimental point, entries in the Hessian $\partial_\alpha \partial_\beta f(\psi_-)$ can be obtained as well, which correspond to interaction energies of solutes in the dilute phase. This is based on the observation that $n_\alpha \propto \sum_{\beta=1}^N k^\beta \partial_\alpha \partial_\beta f(\psi_-)$. To illustrate the point, suppose $\partial_\alpha \partial_\beta f(\psi_-)$ consists of two terms: a constant, symmetric interaction energy matrix $\chi_{\alpha\beta}$ and a diagonal entropic term diag $\left(\frac{1}{L^1\psi_-^1}, \frac{1}{L^2\psi_-^2}, \ldots, \frac{1}{L^N\psi_-^N}\right)$, where L^α are sizes of the solute molecules. In doing so the free energy from translational entropy of solute α is assumed to be $\frac{\psi_-^\alpha}{L^\alpha} \ln \psi_-^\alpha$. Treating the interaction matrix and sizes L^α as unknowns, we have $N(N+1)/2 + N = \frac{1}{2}N^2 + \frac{3}{2}N$ fitting parameters. On the other hand, at each point ψ_-^α, we can form $N-1$ linearly independent equations using ratios of n_α's, so for an N-component system by sampling $\sim \frac{1}{2}N$ points, the interaction constants $\chi_{\alpha\beta}$ and molecular sizes L^α can be deduced. Practical implementation of this procedure can however be difficult, given the possibly large number of relevant solutes, but the prospect of obtaining $\chi_{\alpha\beta}$ in the dilute solution not only helps with understanding phase separation but also illuminates protein interactions in general, and can be a highly promising direction for further research.

Dilute phase response function

The 2-D systems investigated so far serve as illustrative examples of the dominance formulation, and we now return to the realistic scenario where the number of dominant solute species can be more than 2. In addition, concentrations of many of these species can be hard to quantify, so full phase diagrams and tie lines are rarely accessible. We observe, however, that in a typical experiment there will be at least 1 macro-molecular solute whose dilute phase concentration is quantifiable via florescent labelling and microscopy methods [22, 30]. Furthermore, one can also change the total starting concentrations of any solutes, so a quantity of interest is the response $R^\alpha_\beta \equiv \frac{\partial \psi_-^\alpha}{\partial \phi^\beta}$ for a solute α, the concentration of which can be measured in the dilute phase, and for any solute β. It is easily shown via mass conservation that changes in ψ_-^α in response to changes in ϕ^α, evaluated at the phase boundary, can be expressed as (SI section V)

$$\lim_{v\to 0} R^\alpha_\beta = \delta^\alpha_\beta - \frac{n_\beta}{n_\alpha} D^\alpha. \tag{5}$$

The appearance of D^α indicates that only the dominance of α is accessible when the dilute phase concentration of α is measurable, regardless of which solute β is varied to measure the response. Interestingly, by combining two response functions together we can further deduce information on the tie line components k^α and k^β.

In a previous work [22] we established a tie line measurement approach between a solute with index 1 (without loss of generality), and another solute with index 2 through measurement of ψ_-^1 alone, and using the response function formulation we can formalise the approach as asking the following question: how should ϕ^1 and ϕ^2 be changed so that ψ_-^1 stays constant? Mathematically, this requires $\delta\psi_-^1 = 0$ and recall that $\frac{\partial \psi_-^\alpha}{\partial \phi^\beta} \equiv R^\alpha_\beta$ we also have $\delta\psi_-^1 = R^1_1 \delta\phi^1 + R^1_2 \delta\phi^2$. The space defined by $\delta\psi_-^1 = 0$ on the $1-2$ plane is a line, and its gradient is $K^1_2 \equiv \left(\frac{\partial \phi^1}{\partial \phi^2}\right)_{\psi_-^1} = -\frac{R^1_2}{R^1_1}$. Close to the phase boundary we can use Eqs. (4) and (5), after straightforward algebra we arrive at

$$\lim_{v\to 0} K^1_2 = \frac{n_2}{n_1}\frac{D^1}{1-D^1} = \frac{k^1}{k^2}\left[\frac{1}{1+\sum_{\beta\neq 1,2} D^\beta/D^2}\right] \tag{6}$$

and to leading order, K^1_2 provides an approximation of the ratio of tie line components $\frac{k^1}{k^2}$ close to the phase boundary. Terms in the square bracket of Eq. (6) represent the relative deviation of K^1_2 from $\frac{k^1}{k^2}$, and in a true 2-component system we have exactly $\lim_{v\to 0} K^1_2 = \frac{k^1}{k^2}$. On the $1-2$ plane, this line defined by $\delta\psi_-^2 = 0$ can thus be thought of as an N-D tie line 'reduced' to the 2-D plane, and we refer to it as the reduced tie line in the following discussions.

Measuring the gradient of the reduced tie line allows an assessment of the relative solute partitioning to be made. Notably, assuming the dominance of all solutes

fall within the range $(0, 1)$, the sign of K_2^1 is entirely determined by the sign of $\frac{n_2}{n_1}$, and thus the sign of $\frac{k^1}{k^2}$ can be deduced by simply observing the effect of the solute 2 on condensates. To put this in practical terms, if solute 2 dissolves condensates $\left(\frac{n_2}{n_1} < 0\right)$ it partitions out of condensates $\left(\frac{k^1}{k^2} < 0\right)$ and vice versa. This makes intuitive sense since it suggests that condensate-favouring modulators partition into condensates while condensate-disfavouring modulators are excluded from condensates. It is important however to point out here that some D^1 can fall outside the 0 and 1 range, and this can happen when a solute is able to change the chemical potentials of other solutes to make phase separation especially favourable, even though its own energetic contribution is opposing phase separation.

Line-scans as a general, practical approach

We now give practical examples of dominance measurements and interpretation in a range of systems using line-scans. To obtain the dominance of a solute from the dilute phase responses it is necessary to measure its dilute phase concentration and in the following we use the index 1 to denote the solute that is measured. Experimentally, a series of experimental samples can be prepared with varying ϕ^1 or some other ϕ^2 while keeping all other ϕ's constant and measuring ψ_-^1. This corresponds to traversing the phase space in a line parallel to the ϕ^1 or ϕ^2 and the response functions R_1^1 or R_2^1 can be measured. By taking the measurement close to the phase boundary it is convenient to write down the expressions of them again:

$$\begin{aligned} R_1^1 =& 1 - D^1 \\ R_2^1 =& -\frac{n_2}{n_1} D^1 \end{aligned} \tag{7}$$

and we term the former 'homotypic line-scan' and the latter 'heterotypic line-scan', both of which are discussed below.

We take experimental data on phase separation of the optoG3BP1 protein in cells [31] where the dilute phase [optoG3BP1] is measured as a function of total [optoG3BP1], and use the index 1 denotes the optoG3BP1 protein (Figure 4a). We trivially have $R_1^1 = 1$ outside the phase-separated region, and the response becomes modulated beyond some critical value ϕ_c^1. In an ideal 1-D system, for $\phi^1 > \phi_c^1$ we expect $R_1^1 = 0$, while because of the multi-component nature of the system [31] we have $R_1^1 > 0$ for optoG3BP1. Using a 2-segment linear fit for optoG3BP1 data we obtain $D^1 = 0.55 \pm 0.14$. In contrast, in another system involving the protein optoFUS [32], the protein exhibits much more prominent single-component character (Figure 4b) and the dominance of optoFUS is $D^1 = 0.98 \pm 0.07$. This is consistent with the observation that FUS phase separates easily on its own [33, 34] and can be less reliant on other components compared to G3BP1, where other macromolecules such as RNA are typically added to G3BP1 solution to trigger phase separation [8, 35]. A simple dominance measurement thus allows a quick assessment of the multi-component character of a system to be made, and next we explore how it responds to addition of modulators.

Poly(A)-RNA phase separates in the presence of PEG and at high [KCl] [24, 36], and here we investigate how the dominance of poly(A) changes upon addition of salt. We perform homotypic line-scans with 4% PEG (molecular weight 10 kilodaltons), and 800mM or 850mM of KCl (SI section VI). Dilute phase poly(A) concentrations are measured, so we use index 1 to denote poly(A) and index 2 for KCl, and denote the difference in total KCl concentrations as $\Delta\phi^2 = 50$mM. Line-scan data (Figure 4c) shows a smaller R_1^1 after phase-separation at higher KCl so D^1 increases from 0.49 ± 0.05 to 0.66 ± 0.04. The increase in poly(A) dominance at higher KCl can be explained by the increased screening of negative backbone charges on poly(A), facilitating poly(A)/poly(A) interaction and rendering other interactions, for instance poly(A)/PEG, less significant. An interesting observation is that the onset of phase-separation shifts to a lower poly(A) concentration when salt concentration is increased, with $\Delta\phi_c^1 = -0.54 \pm 0.12$g/l. This can be interpreted as an increase in overall phase-separation propensity, consistent with the picture that poly(A)/poly(A) repulsion weakens with more salt. By combining $\Delta\phi^2$ with $\Delta\phi_c^1$ we can deduce the ratio of surface normals $\frac{n_2}{n_1}$ in the poly(A)-KCl plane (Figure 4d). By definition, $n_1\Delta\phi_c^1 + n_2\Delta\phi^2 = 0$ so

$$\frac{n_2}{n_1} = -\frac{\Delta\phi_c^1}{\Delta\phi^2} \tag{8}$$

and this gives $\frac{n_2}{n_1} = -\frac{\Delta\phi_c^1}{\Delta\phi^2} = 10.8 \pm 2.4 \frac{\text{g/l}}{\text{M}}$. By combining this with the average D^1, we can further calculate the gradient of the reduced tie line as $K_2^1 = 9.4 \pm 1.8 \frac{\text{g/l}}{\text{M}}$, so KCl partitions into poly(A) condensates.

A subtle point here in calculating K_2^1 involving KCl is that the dissociation of the salt into K^+ and Cl^- means that KCl is not a single solute, and the line-scan is not traversing parallel to one axis but at an angle between two axes corresponding to K^+ and Cl^-, so mixing them is equivalent to performing a rotation of the two axes. This does not affect $D^1 = \frac{n_1 k^1}{\sum_{\gamma=1}^N n_\gamma k^\gamma}$ since the denominator is coordinate-independent and the numerator is not affected. Furthermore, since k^α and ϕ^α transform in the same way the measured K_2^1 represents the summed partitioning of K^+ and Cl^-.

The homotypic line-scan is a natural path towards conceptualising D^1, while in experiments the heterotypic line-scan can also be performed [20, 22]. To simply illustrate the approach again we take two sets of data:

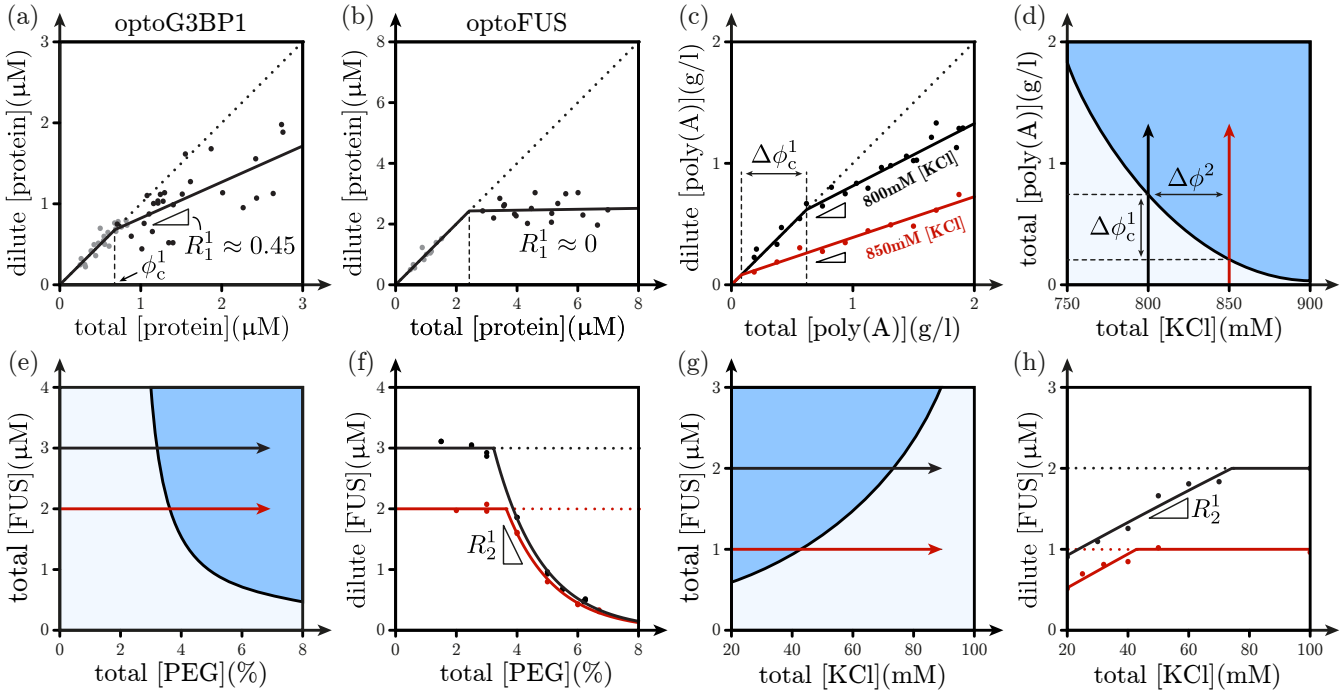

FIG. 4. (a) The dilute phase response of optoG3BP1 [31] exhibits multi-component character, with $D^1 = 1 - R_1^1 = 0.55 \pm 0.14$. (b) In the optoFUS system [32] the protein has much stronger single-component character. (c) Line-scan data for phase-separation of poly(A)-RNA in the presence of PEG and KCl. At higher [KCl] the increased charge screening allows inter-RNA interaction to be more favourable, leading to an increase in D^1 when [KCl] is increased. (d) Phase space illustration of the poly(A)-KCl cross-section. (e) Illustration of heterotypic line-scan sampling in a 2-D cross-section of the FUS-PEG phase space. Line-scans are performed at two fixed FUS concentrations, 3μM and 2μM. (f) Data from [22]. At low [PEG] no phase separation is observed, so the dilute phase [FUS] is simply a constant. When the line-scan trajectory enters the phase separated region the dilute phase [FUS] starts decreasing, and this initial gradient is taken as R_2^1. (g) Phase space illustration of the FUS-KCl line-scans. KCl dissolves condensates, in contrast to PEG. (h) Data from [20]. Scatter points are data and solid lines are phenomenological fits. Dotted lines indicate trivial results in the absence of phase-separation.

FUS/PEG from [22] and FUS/KCl from [20]. In both cases dilute phase FUS protein (index 1) concentration is measured, while the total concentrations of PEG or KCl (index 2) is varied. In the FUS/PEG line-scan data from [22], two line-scans are performed at 2 and 3μM [FUS] while adding PEG up to 8% weight fraction. The dilute phase [FUS] measurements showed a plateau at low [PEG] and an exponential decrease as some thresholding [PEG] is reached (Figure 4e and 4f). The two points at the onset of the decrease are where the lines cross the phase boundary, and from these we estimate $\frac{n_2}{n_1} = 2.4 \pm 0.4 \frac{\mu\text{M}}{\%}$. The response function R_2^1 can be evaluated at the drop-off point as well, giving $D^1 = 0.78 \pm 0.15$ at 3μM [FUS] and low [PEG] and $D^1 = 0.52 \pm 0.10$ at 2μM [FUS] and high [PEG]. These dominance values indicate there are other solutes actively participating in phase-separation and a likely candidate is PEG. This is also reflected in the fact that the FUS/PEG phase boundary measured using PhaseScan has strong dependence on [PEG] [37]. Treating PEG as a modulator, the addition of PEG thus leads to a decrease in FUS dominance and at the same time a decrease in the critical FUS concentration. A plausible explanation of this is that PEG itself has strong phase separation propensity, so addition PEG both drives phase separation and at the same time pushes the system to mimic a case where it is just PEG phase separating and FUS is becoming irrelevant. Substituting $\frac{n_1}{n_2}$ and the average D^1 into Eq. (6) we get $K_2^1 = 4.5 \pm 1.8 \frac{\mu\text{M}}{\%}$, providing an estimate of the relative partitioning between FUS and PEG. In the FUS/KCl system [20], KCl has the opposite effect compared to PEG as condensates are dissolved when more KCl is added to the system [20]. Line-scan data thus shows a steady increase of dilute phase [FUS] with increasing [KCl] (Figure 4g and 4h). We fit the dilute phase [FUS] after phase-separation using a linear function. Repeating the same calculations we obtain $\frac{n_2}{n_1} = -0.033 \pm 0.009 \frac{\mu\text{M}}{\text{mM}}$ and $R_2^1 = 0.020 \pm 0.003 \frac{\mu\text{M}}{\text{mM}}$ to give $D^1 = 0.61 \pm 0.24$, again suggesting a FUS-dominated, multi-component system. The R_2^1 value for the two scans are similar so here we only calculate the average of the dominances. The K_2^1 value obtained is $K_2^1 = -0.05 \pm 0.04 \frac{\mu\text{M}}{\text{mM}}$, implying overall salt is partitioning outside condensates. Heterotypic line-scans are thus an alternative to homotypic line-scans, and the two methods can have different

signal-to-noise ratios depending on the phase space being probed. In general, for a solute α with a small D^α, heterotypic line-scans give more robust readouts and conversely, homotypic line-scan should be performed when D^α is large.

Conclusion

To summarise, we have formulated a dimensionless parameter D^α to quantify the dominance of solutes in a binary phase separation system based on their contribution to the stabilisation free energy, and showed that it can be experimentally measured by quantifying the phase boundary and tie lines, or the dilute phase concentration response of a solute. This framework also engenders the concept of reduced tie lines that is closely related to the ratio of true tie line components. By measuring the dominance parameter, insights regarding interactions driving phase separation and actions of modulators can be gained. Furthermore, the dimensionless nature of the dominance allows direct comparison between solutes of distinct properties, for instance it will be possible to compare the dominance of a macromolecular solute with that of a small molecule species, if the dilute phase concentration of the latter can be measured. The dominance framework thus leads to many more directions of future research.

Acknowledgement

The authors thank Mina Farag for helpful discussions. The research leading to these results has received funding from Global Research Technologies, Novo Nordisk A/S (H.A., T.P.J.K.), the European Research Council under the European Union's Horizon 2020 research and innovation programme through the Marie Skłodowska-Curie grant MicroREvolution (agreement ID 101023060; T.S.), the Newman Foundation (T.S., T.P.J.K.), and the European Research Council under the European Union's Horizon 2020 research and innovation program through the ERC grant DiProPhys (agreement ID 101001615; T.P.J.K.).

Conflict of interests

The authors declare no conflict of interests.

[1] J. W. Gibbs, American Journal of Science and Arts **16**, 441 (1874).

[2] S. F. Banani, H. O. Lee, A. A. Hyman, and M. K. Rosen, Nature Reviews Molecular Cell Biology **18**, 285 (2017).

[3] Y. Shin and C. P. Brangwynne, Science **357**, aaf4382 (2017).

[4] G. L. Dignon, R. B. Best, and J. Mittal, Annual Review of Physical Chemistry **71**, 53 (2020).

[5] C. P. Brangwynne, C. R. Eckmann, D. S. Courson, A. Rybarska, C. Hoege, J. Gharakhani, F. Jülicher, and A. A. Hyman, Science **324**, 1729 (2009).

[6] B. A. Gibson, L. K. Doolittle, M. W. Schneider, L. E. Jensen, N. Gamarra, L. Henry, D. W. Gerlich, S. Redding, and M. K. Rosen, Cell **179**, 470 (2019).

[7] A. Aulas, G. Caron, C. G. Gkogkas, N. V. Mohamed, L. Destroismaisons, N. Sonenberg, N. Leclerc, J. Alex Parker, and C. V. Velde, Journal of Cell Biology **209**, 73 (2015).

[8] J. Guillén-Boixet, A. Kopach, A. S. Holehouse, S. Wittmann, M. Jahnel, R. Schlüßler, K. Kim, I. R. Trussina, J. Wang, D. Mateju, I. Poser, S. Maharana, M. Ruer-Gruß, D. Richter, X. Zhang, Y.-T. Chang, J. Guck, A. Honigmann, J. Mahamid, A. A. Hyman, R. V. Pappu, S. Alberti, and T. M. Franzmann, Cell **181**, 346 (2020).

[9] J. E. Henninger, O. Oksuz, K. Shrinivas, I. Sagi, G. LeRoy, M. M. Zheng, J. O. Andrews, A. V. Zamudio, C. Lazaris, N. M. Hannett, T. I. Lee, P. A. Sharp, I. I. Cissé, A. K. Chakraborty, and R. A. Young, Cell **184**, 207 (2021).

[10] S. Ray, N. Singh, R. Kumar, K. Patel, S. Pandey, D. Datta, J. Mahato, R. Panigrahi, A. Navalkar, S. Mehra, L. Gadhe, D. Chatterjee, A. S. Sawner, S. Maiti, S. Bhatia, J. A. Gerez, A. Chowdhury, A. Kumar, R. Padinhateeri, R. Riek, G. Krishnamoorthy, and S. K. Maji, Nature Chemistry **12**, 705 (2020).

[11] A. Patel, H. O. Lee, L. Jawerth, S. Maharana, M. Jahnel, M. Y. Hein, S. Stoynov, J. Mahamid, S. Saha, T. M. Franzmann, A. Pozniakovski, I. Poser, N. Maghelli, L. A. Royer, M. Weigert, E. W. Myers, S. Grill, D. Drechsel, A. A. Hyman, and S. Alberti, Cell **162**, 1066 (2015).

[12] J. McCarty, K. T. Delaney, S. P. Danielsen, G. H. Fredrickson, and J. E. Shea, Journal of Physical Chemistry Letters **10**, 1644 (2019).

[13] S. Mao, D. Kuldinow, M. P. Haataja, and A. Košmrlj, Soft Matter **15**, 1297 (2019), arXiv:1810.03689.

[14] M. Heidenreich, J. M. Georgeson, E. Locatelli, L. Rovigatti, S. K. Nandi, A. Steinberg, Y. Nadav, E. Shimoni, S. A. Safran, J. P. Doye, and E. D. Levy, Nature Chemical Biology **16**, 939 (2020).

[15] M. Farag, S. R. Cohen, W. M. Borcherds, A. Bremer, T. Mittag, and R. V. Pappu, Nature Communications **13**, 7722 (2022), arXiv:2022.05.21.492916 [10.1101].

[16] M. Farag, W. M. Borcherds, A. Bremer, T. Mittag, and R. V. Pappu, (2023).

[17] M. Kar, L. T. Vogel, G. Chauhan, H. Ausserwöger, T. J. Welsh, A. R. Kamath, T. P. J. Knowles, A. A. Hyman, C. A. M. Seidel, and R. V. Pappu, (2023).

[18] V. G. Taratuta, A. Holschbach, G. M. Thurston, D. Blankschtein, and G. B. Benedek, Journal of Physical Chemistry **94**, 2140 (1990).

[19] A. Testa, M. Dindo, A. A. Rebane, B. Nasouri, R. W. Style, R. Golestanian, E. R. Dufresne, and P. Laurino, Nature Communications **12**, 1 (2021).

[20] H. Ausserwoger, D. Qian, G. Krainer, T. J. Welsh, T. Sneideris, T. M. Franzmann, S. Qamar, J. Nixon-Abell, M. Kar, P. S. G. Hyslop, A. A. Hyman, S. Alberti, R. V. Pappu, and Tuomas P. J. Knowles, bioRxiv (2023).

[21] A. A. André and E. Spruijt, International Journal of Molecular Sciences **21**, 1 (2020).

[22] D. Qian, T. J. Welsh, N. A. Erkamp, S. Qamar, J. Nixon-Abell, G. Krainer, P. St. George-Hyslop, T. C. T. Michaels, and T. P. J. Knowles, Physical Review X **12**, 041038 (2022), arXiv:2022.02.22.481401 [10.1101].

[23] A. A. André, N. A. Yewdall, and E. Spruijt, Biophysical Journal **122**, 397 (2023).

[24] N. Erkamp, M. Farag, D. Qian, T. Sneideris, T. Welsh, H. Ausserwoger, D. Weitz, R. Pappu, and T. Knowles, , 1 (2023), arXiv:2023.01.12.523837.

[25] M. L. Huggins, The Journal of Chemical Physics **9**, 440 (1941).

[26] P. J. Flory, The Journal of Chemical Physics **10**, 51 (1942).

[27] D. D. Lee, J. H. Choy, and J. K. Lee, Journal of Phase Equilibria **13**, 365 (1992).

[28] J. Wolff, C. M. Marques, and F. Thalmann, Physical Review Letters **106**, 1 (2011).

[29] J.-M. Choi, F. Dar, and R. V. Pappu, PLOS Computational Biology **15**, e1007028 (2019).

[30] A. Bremer, M. Farag, W. M. Borcherds, I. Peran, E. W. Martin, R. V. Pappu, and T. Mittag, Nature Chemistry (2021), 10.1038/s41557-021-00840-w.

[31] J. A. Riback, L. Zhu, M. C. Ferrolino, M. Tolbert, D. M. Mitrea, D. W. Sanders, M. T. Wei, R. W. Kriwacki, and C. P. Brangwynne, Nature **581**, 209 (2020).

[32] M. T. Wei, Y. C. Chang, S. F. Shimobayashi, Y. Shin, A. R. Strom, and C. P. Brangwynne, Nature Cell Biology **22**, 1187 (2020).

[33] M. Kar, F. Dar, T. J. Welsh, L. T. Vogel, R. Kühnemuth, A. Majumdar, G. Krainer, T. M. Franzmann, S. Alberti, C. A. Seidel, T. P. Knowles, A. A. Hyman, and R. V. Pappu, Proceedings of the National Academy of Sciences of the United States of America **119**, 1 (2022).

[34] G. Krainer, T. J. Welsh, J. A. Joseph, J. R. Espinosa, S. Wittmann, E. de Csilléry, A. Sridhar, Z. Toprakcioglu, G. Gudiškytė, M. A. Czekalska, W. E. Arter, J. Guillén-Boixet, T. M. Franzmann, S. Qamar, P. S. George-Hyslop, A. A. Hyman, R. Collepardo-Guevara, S. Alberti, and T. P. J. Knowles, Nature Communications **12**, 1085 (2021).

[35] P. Yang, C. Mathieu, R. M. Kolaitis, P. Zhang, J. Messing, U. Yurtsever, Z. Yang, J. Wu, Y. Li, Q. Pan, J. Yu, E. W. Martin, T. Mittag, H. J. Kim, and J. P. Taylor, Cell **181**, 325 (2020).

[36] N. A. Erkamp, T. Sneideris, H. Ausserwöger, D. Qian, S. Qamar, J. Nixon-Abell, P. St George-Hyslop, J. D. Schmit, D. A. Weitz, and T. P. J. Knowles, Nature Communications **14**, 684 (2023).

[37] W. E. Arter, R. Qi, N. A. Erkamp, G. Krainer, K. Didi, T. J. Welsh, J. Acker, J. Nixon-Abell, S. Qamar, J. Guillén-Boixet, T. M. Franzmann, D. Kuster, A. A.

Hyman, A. Borodavka, P. S. George-Hyslop, S. Alberti, and T. P. J. Knowles, Nature Communications **13**, 7845 (2022).